

# Numerical Simulation of Glider Winch Launches

Andreas Gäb and Christoph Santel  
Institute of Flight System Dynamics, RWTH Aachen University  
Willnerstr. 7, 52062 Aachen, Germany  
gaeb@fsd.rwth-aachen.de

Presented at the XXX OSTIV Congress, Szeged, Hungary, 28 July - 4 August 2010

## Abstract

This paper describes a Matlab/Simulink framework for simulating the winch launching of gliders that has been realized and employed for a number of analyses. It comprises models of the aircraft, pilot, winch, winch operator, cable, atmosphere and terrain. Modeling of these building blocks is described in detail. Results are presented for analyses of a reference case, wind influence and overly steep initial climbs.

## Nomenclature

$A$	Area
$c$	Spring constant
$d$	Damper constant
$E$	Elastic modulus
$F$	Force
$g$	Gravitational acceleration
$k$	Controller gain factor, indexed by controller output and input values
$m$	Mass
$p$	Roll rate
$q$	Dynamic pressure
$s$	Spring/damper compression length
$T$	Tension force
$x$	Longitudinal position
$z$	Vertical position (negative altitude)
$\beta$	Angle of sideslip
$\varepsilon$	Extension
$\mu$	Friction coefficient
$\zeta$	Aileron deflection
$\Phi$	Bank angle
$\chi$	Flight path azimuth

## Indices

$C$	Commanded value
$CP$	Contact point
$D$	Drag
$F$	Friction
$j$	Index of finite cable element
$S$	Spring-damper
$R$	Reaction

## Introduction

The most common way of launching a sailplane in Europe is the winch launch. Practical experience on this subject, therefore, is abundant and some theoretical works are available, most notably König's 1978 article<sup>1</sup>. A few attempts have been made at simulating the winch launch. However, those

available all had certain limitations, e.g. restriction to longitudinal motion of a single aircraft type or the exclusion of wind influence.

The Department of Flight Dynamics at RWTH Aachen University has developed a generic six degree of freedom aircraft simulation which was extended to allow for the simulation of glider winch launches in arbitrary wind conditions in longitudinal as well as lateral motion. The extension is described in detail by Santel<sup>2</sup>.

## Simulated procedure

Regulations on sailplane operating procedures such as the German "Segelflugsportbetriebsordnung" (SBO) or the "Laws and Rules" of the British Gliding Association contain little information on how to actually carry out a winch launch. Piloting as well as winch operation practices are usually learned by experience in the gliding clubs. However, recent discussion of winch launch safety, especially in Germany<sup>3</sup>, recommended that exclusively the pilot controls airspeed (with the elevator) while the winch operator should command and control a constant winch force during climb. Still, the winch force must be moderate in the beginning of the launch sequence to avoid over-rotation at liftoff<sup>4</sup>.

This is not the most common practice at the moment, especially as measurement equipment for cable force is available on only a few legacy winches. However, as benefits in safety as well as in altitude gain can be expected, this procedure was chosen as reference case for this paper. Also, contemporary electrical winches offer built in force control by default, thus this approach probably will become more common in the future.

## The simulation framework

The simulation framework was implemented in the Matlab/Simulink environment. It consists of the main Simulink model, including the building blocks described below and a set of Matlab scripts to operate the model. A graphical-user-interface (GUI) allows specifying input parameters and easily

displaying simulation results. It was decided not to resort to Mathworks' official aerospace toolbox and blockset, but to make use of the Embedded Matlab functionality. This increased execution speed and allowed various equations to be formulated in code instead of block diagrams, which was deemed to increase readability and maintainability.

The winch launch simulation is one part of general framework. The framework also is used for other applications ranging from the presentation of aircraft eigenmotions to students in lectures to analyzing flying qualities during the design process of micro aerial vehicles.

### Aircraft

The aircraft model is based on the simulation used for a former study<sup>5</sup>. Since then, its configuration has been made more generic to allow for easier modeling of different aircraft.

The aircraft block contains the equations of motion, which in this case are those for a rigid body moving in six degrees of freedom over an Earth approximated to be flat and non-rotating. For the short distances covered during a winch launch, this approximation is well justified.

Forces and moments acting on the aircraft arise from aerodynamics, ground reactions, external sources (the cable), the weight and possibly propulsion. The aerodynamic model is formulated as coefficient lookup tables for the whole aircraft.

The aircraft used for the analyses in this paper corresponds to a Schleicher ASK 21 two-seat training glider. Data for the aerodynamics and inertia are taken from the flight tests described in Ref. 5, although some simplifications (e.g. a parabolic polar, quasi-steady airflow) were made. A basic ground effect model was included which applies panel methods as no ground effect flight data was available.

### Pilot

The human pilot is modeled by elements from linear control theory. The pilot model is assigned three main tasks:

1. Maintain airspeed using the elevator
2. Maintain ground track using the ailerons
3. Minimize angle of sideslip using the rudder.

Thus, the model is divided into three independent channels, one for each task. Each channel comprises at least a PID (proportional, integral + derivative) controller as the main element and a proportional damper. The aileron channel consists of two nested loops for ground track and bank angle. All controller gains are scheduled by scaling with the inverse of dynamic pressure to adapt surface deflections to the airspeed.

Human factors are considered in the form of reaction time (a fixed delay (dead time) element) and neuromuscular delay (a first order delay element).

As an example, the aileron controller is depicted in Fig. 1. The actual flight path azimuth  $\chi$  is subtracted from the commanded value  $\chi_C$  to yield an azimuth error. A weighted sum of this error, its integral and its time derivative (P, I, D) is taken as the commanded value for the bank angle  $\Phi_C$ . Subtraction of

the actual bank angle gives the bank angle error, which multiplied by a gain  $k_{\xi\Phi}$  to give one component of the commanded aileron deflection angle  $\xi$ . The other component is the roll rate  $p$ , multiplied by another gain  $k_{\xi p}$  (roll damper). The final commanded aileron deflection angle is multiplied by the ratio of the reference dynamic pressure  $q_C$  to the actual dynamic pressure  $q$  to account for varying aileron efficiency due to varying airspeed. Finally, and not shown in the figure, the human factor elements are applied to the commanded aileron deflection.

For all controllers, authority is faded in smoothly after reaching a safety altitude. That means that during the initial phase of the launch, all surfaces are kept fixed with ailerons and rudder centered and elevator in trim deflection.

One has to keep in mind that a control-theory based description of human behavior only can consider certain aspects of the complex human decision making process. While visual feedback information is available to the pilot in the elevator and rudder channels, with both the airspeed indicator and the yaw string being in the pilot's field of vision, no such information is available in the aileron channel. With the glider being pitched upwards during the main climb phase, the glider pilot lacks any reference points in the direction of flight by which to gauge his azimuth / heading or ground track. Hence, the glider pilot will usually select his roll angle by experience, a process more adequately described by feed-forward control or fuzzy logic. Also, in the elevator channel, speed is not the only objective the pilot controls. Especially at the end of the launch, pitch angle becomes important as well. Such extensions were beyond the scope of this project, thus they are not considered in this contribution.

### Winch

The winch is modeled by a simple drive train model as used in automotive engineering. The internal combustion engine represented by its characteristic diagram (maximum power over RPM). All rotating elements are reduced to the drum shaft, so they can be replaced by a single flywheel. Due to its moment of inertia, this flywheel acts as an energy accumulator. Energy may be added by the engine or drained by the cable.

All losses within the winch are subsumed into a single degree of efficiency. Detailed component modeling was not undertaken of clutches, torque converters or throttle mechanics/dynamics. Engine power was proportional to throttle position. This is only a first order approximation for piston engines. A more accurate modeling was not undertaken.

The specific winch modeled in this paper has a GM Duro-max 6.6L turbocharged diesel engine with a 0.7 m diameter drum, corresponding roughly to a Skylaunch 3 winch.

### Winch operator

The winch operator controls the winch force using the engine throttle. The model contains a PID controller and the

same human factors model as the pilot model. The commanded force to be adhered to depends on time. It starts from an initial value and is raised to the maximum value after lift-off or during full climb. Until reaching a maximum cable angle, the force is kept constant and afterwards released again smoothly to allow a soft cable release.

As mentioned above, force control is not an easy task for the operator of a piston-powered winch, and as the pilot in crosswind conditions, they would mainly have to resort to feed-forward control. Again, more accurate modeling of the human decision making process was beyond the scope of this project.

### Cable

Two cable models may be selected in the simulation:

1. A simple secant model without force variations along the cable.
2. An FEM cable model including internal and external cable forces.

The secant model was introduced mainly for development purposes. However, as it significantly reduces calculation times, it can still be used for “quick-and-dirty” tests. It neglects all cable dynamics and simply applies a force at the glider hook whose magnitude corresponds to the winch force and which points directly towards the winch. This approach may be regarded as the physical limit for a cable without external forces (aerodynamic drag, ground reaction forces) and mass.

The full FEM model is based on the work in Ref. 7 and utilized in Ref. 2. It divides the cable into a set of mass points which are connected by mass-less cylinders. The cylinders are subject to external forces (aerodynamic drag). Their elasticity is modeled with spring and damping constants, yielding the cable tension as an internal force. The mass points experience weight and possibly ground reaction forces. Figure 2 shows a schematic of the forces.

The extension  $\varepsilon$  of the cable is determined from the relative distances of the mass points. Its time derivative yields the extension speed. Using these, the tension  $T$  in the  $j$ th cable element is calculated as

$$T_j = A(E\varepsilon_j + d\dot{\varepsilon}_j) \quad (1)$$

with  $A$  being the cable cross section area,  $E$  its elastic modulus and  $d$  a damping factor. The tension acts along the direction of the cable element. The winch force is introduced as boundary condition for the tension at the lower end of the cable, while the tension at the higher end is the external force acting at the glider. Boundary conditions for the position are, respectively, the winch drum and tow hook locations.

Aerodynamic drag on the cable elements is split into normal and tangential components according to Ref. 7, where the component magnitudes are dependent on total angle of attack.

Drag is assumed to act at the middle of the cylinders, so the drag force acting on the mass points is the mean of the drag forces on the respective adjacent cylinders.

Thus the acceleration of each mass point, corresponding to the total force acting on it, is calculated as

$$\ddot{\vec{r}}_j = \frac{1}{m_j} (\vec{F}_{ext} + \vec{T}_j + \vec{T}_{j-1}) \quad (2)$$

where  $F_{ext}$  is the external force consisting of weight  $m_j g$ , drag and ground reaction force  $F_R$  as calculated using Eq. (6):

$$\vec{F}_{ext} = m_j \vec{g} + \frac{1}{2} (\vec{F}_{D,j-1} + \vec{F}_{D,j}) + \vec{F}_{R,j} \quad (3)$$

The mass points are allowed to move according to the forces acting on them. In other words, the sum of forces scaled by mass is integrated once to yield the velocity of the mass point and a second time for its position. Rotational degrees of freedom of mass points and cable cylinders are neglected. As tension is by far the dominant force, lateral excursions are minimal.

Different types of cable (synthetic material or steel) are modeled by the properties  $m$ ,  $A$ ,  $E$  and  $d$ ; and when no manufacturer’s data is available, estimates must be made.

The simulation starts with a maximum number of FEM elements, usually 20. The reeling of the cable is approximated by sequentially removing single FEM elements when they approach the winch location. When one element is removed, the winch force is introduced as boundary condition for the next element and forces on the removed element are set to zero. This allows continued integration of the equations of motion for the removed elements, thus avoiding a varying number of states in the Simulink model.

### Ground reactions

Ground reactions are assumed to take place only at specific contact points as shown in Fig. 3. At each of these points, a spring-damper-combination subject to friction is used to calculate the force.

The contact points may be wheels, skids, exposed structure elements like wingtips or the mass points of the cable model. If any of the contact points is below local ground level, reaction forces for this point are calculated. It is assumed that the amount by which the contact point is below the ground corresponds to the spring deflection  $s$ . The time derivative of this length is the deflection speed  $\dot{s}$ .

The spring-damper force is given by the equation:

$$F_s = c \cdot s + d \cdot \dot{s} \quad (4)$$

where  $c$  is the spring constant and  $d$  is the damping constant.  $F_R$  is assumed to act along the direction of the local vertical. It is zero when the contact point is above the ground.

The friction force in the local horizontal plane is attained by multiplication with the friction coefficient

$$F_F = \mu \cdot F_S \quad (5)$$

The friction force is assumed to act against the direction of the local velocity in the ground plane, characterized by the contact point azimuth angle  $\chi_{CP}$ . The total reaction force vector acting on the contact point, thus, is calculated as

$$F_R = (F_F \sin \chi_{CP}, F_F \cos \chi_{CP}, F_S)^T \quad (6)$$

The total reaction force vector is expressed in the local-level frame. As of now, the contact point model includes only a single friction coefficient, and no distinction is made between static, dynamic or rolling friction.

### Atmosphere

The basic atmosphere model is the International Standard Atmosphere. As an extension, wind and turbulence (in form of stochastic noise and/or deterministic gusts) are modeled. Wind is assumed to be of equal magnitude and direction along the whole cable and at the aircraft.

### Numerical issues

The main model carries out the integration of the equations of motion of the aircraft, the cable mass points and the winch. For aircraft without external forces, this integration is numerically well-behaved with time steps up to 20 ms; however, the cable model affects numerical stability in a strongly negative manner due to the elastic modes of the cable. As their frequency is much higher than the eigenmotions of the aircraft, the overall system is much stiffer than the aircraft model alone. The ratio from maximum to minimum eigenvalue jumps from about  $10^3$  to  $10^9$ .

Simple Euler integration needs time steps of less than 1 ms, and the 4th order Runge-Kutta method requires time steps of 10 ms or less for a cable with 20 mass points. The aircraft model alone may be run at a time step of 20 ms with the Euler method.

## Results of analyses

### Reference case

The reference case for the analyses was the launch of a training two-seater, comparable to the Schleicher ASK 21, with 1000 m of synthetic cable, without any wind and using the default settings for all subsystems. The simulation starts with the winch running but the glider at rest on ground.

According to the ASK 21 flight manual, the recommended speed during the winch launch is 25 to 30 m/s (90-110 km/h or 50-60 knots), while 42 m/s (150 km/h, 80 knots) is not to be exceeded. The upper limit of recommended speeds was chosen as the target speed to increase the safety margin with respect to the stalling speed. It is only slightly above the minimum speed recommended by Eppler<sup>3</sup>, which is 29.3 m/s for this case.

The winch force starts at a value of 2500 N, corresponding to roughly one half of the glider weight. It is increased after liftoff within 5 s to 7500 N (1.5 times the weight or 75% of the breaking force of the weak link) and decreased again when reaching a cable angle of 65 degrees. Target force and actual cable force acting onto the glider are shown in Fig. 4.

In this case, the glider reaches an altitude of 431 m after 35 s of winching. Figure 5 shows the flight path, with the cable position added for one time step to illustrate the cable sag captured by the FEM model. The airspeed during the launch is given in Fig. 6. Its steady increase slows a bit after liftoff, as part of the available power goes into increasing potential rather than kinetic energy. About 10 s after beginning of the ground roll, the safety altitude is reached and the pilot controller activates, rotating the aircraft and bringing airspeed down to near the commanded value. It should be noted that the exact commanded value is not reached due to the continuous “disturbance” of the cable force. A different choice of controller gains could alleviate this, as the elevator has not yet reached its hard stop. However, then the controller performance in the initial flight state worsens.

The speed is at least 25% above the stalling speed during the critical early phases of the launch. Stalling speed is a direct function of the aerodynamic load factor (lift over weight), whose time history is plotted in Fig. 7, along with the cable load factor (cable force over weight) and the vertical load factor perceived by the pilot (actual vertical acceleration over gravitational acceleration), which is considerably lower than the aerodynamic load factor, as lift and cable force partly cancel each other.

During the climb, the aerodynamic load factor and the stalling speed increase along with the cable angle. Therefore, the airspeed safety margin decreases, as the airspeed controller maintains constant speed. This should be kept in mind in real operations. However, pilots are trained to push the nose down at the end of the launch to allow for a soft release, which automatically increases airspeed and alleviates the problem.

The reference case constitutes an example for a safe winch launch in accordance with the practices recommended by Eppler<sup>3</sup>. It will now be compared against some varying situations arising from different environment or pilot/operator behavior.

### Effects of wind

Days without any wind tend to be rare in real life, therefore wind models have been incorporated into the simulation. The effects of a headwind, a tailwind and crosswinds were studied.

As can be seen in the flight paths of Fig. 8, headwind increases the release altitude with the same cable lengths, and the launching takes more time. The opposite is true for tailwinds. The effect of wind on altitude and release time is shown in Fig. 9. A gradient of roughly 5 m altitude per km/h wind speed can be observed. Airspeed and stalling speed have similar time histories as in the case without wind and, therefore, are not shown in a figure. However, it can be noted that tailwinds do not significantly reduce the safety margin, at least if the pilot manages to accurately control the airspeed. For real life pilots, this might prove difficult as they are used to much lower ground speeds from the usual case of non-tailwind launches. The same holds for crosswinds, which also did not have a noticeable effect on release altitude.

### “Kavalierstart”

The German colloquial term “Kavalierstart” refers to an excessively steep initial launch attitude which is known to be dangerous but still tends to happen. It can either be consciously effected by the pilot (by pulling on the stick too early and too much in an attempt to gain more altitude) or occur unintended as a result of too strong a winch force for a given glider. Both versions have been simulated, as well as the combination of both. The simulated Kavalier pilot pulls back the elevator to the hard stop swiftly after lift off, while the simulated Kavalier winch operator increases the winch force to the maximum during ground roll.

The resulting flight paths are shown in Fig. 10. It is obvious that the Kavalier pilot’s attempt to gain more altitude is futile; the release is less than 10 m higher than in the reference case. The Kavalier winch operator, however, can increase the altitude significantly, as the total amount of energy being added into the system is much higher. But, the pilot has to pay a price for this, as can be seen in Fig. 11, which shows true airspeed, stalling speed and the safety margin  $S$  defined as

$$S = \frac{V_{TAS} - V_{stall}}{V_{stall}} \cdot 100\% \quad (7)$$

(For the calculation of  $S$ , true airspeeds are used as they are readily available in the simulation. A real life pilot is of course usually only provided with the indicated airspeed).

If the pilot decides not to counteract the strong force by pulling on the stick, his airspeed will significantly overshoot the allowable airspeed in winch launch, risking damage to the aircraft structure. On the other hand, if the pilot pulls to maintain airspeed, the safety margin to the stalling speed is reduced significantly, down to as low as 11%, while in the reference case the minimum in the initial phase is 26%. The reduction of safety margin is visible in all types of Kavalierstart, illustrating the inherent danger in all of them.

### Summary

The paper describes a simulation framework for the winch launch of gliders and presents results produced with it. The simulation comprises various building blocks which are described in detail. The pilot model is divided into separate channels for elevator, aileron and rudder, which are built by linear control theory elements. Although some extensions might be desirable, the controller approximates real pilot behavior reasonably well.

The winch model is fairly simple, consisting of a drum and an attached engine being characterized by its power curve. The winch operator is said to control the cable force with the engine throttle, being again modeled by linear control theory elements.

The most sophisticated model in the simulation is the cable model. The cable is discretized into finite elements which experience tension forces from their neighbors, aerodynamic drag, weight and possibly reaction forces from ground contact. The equations of motion are solved individually for each finite element. Reeling of the elements is also simulated.

During the simulated launch, the pilot controls his airspeed with the elevator while the winch operator provides a constant cable force. In the reference case it is shown that – provided adequate airspeeds and winch forces are chosen – leads to a safe launch considering safety margin to stall speed.

The effect of head- and tailwinds on the release altitude is shown, where a gradient of about 5 m altitude per km/h headwind can be found.

Finally, the “Kavalierstart” (too steep initial climb) is analyzed. The safety margin against stalling is strongly reduced in this case, be it induced by the pilot or the winch operator. Thus, both concerned persons carry a responsibility of avoiding this hazardous situation: the winch operator by starting the launch with moderate forces and increasing them only gently; the pilot by keeping the airspeed in a safe range above the stalling speed, while avoiding excessive pitch angles.

### Outlook

A current diploma thesis<sup>6</sup> at the Department of Flight Dynamics concerns the investigation of accidents occurring during the winch launch. Here, particular attention is paid to a series of accidents where modern gliders have rolled inverted at low altitude and then impacted the ground with a significant nose down attitude, often resulting in serious or fatal injury to the flight crew. A current hypothesis is that asymmetric dynamic stall effects are responsible for the highly dynamic maneuvering preceding impact. To analyze these effects in more detail, a multi-points aerodynamics model – based on blade element theory – is currently being developed. This will allow for the study of span-wise changes in the aerodynamic conditions.

Further possible extensions concern the winch model where especially engine throttle dynamics and a torque converter could improve fidelity. A sophisticated model of an electric winch would allow comparisons against the piston engines.

### References

- <sup>1</sup>König, U.: "Theorie des Windenstarts", *Aerokurier*, Vol. 1, 1978, pp. 32 – 35.
- <sup>2</sup>Santel, C.: "Numeric simulation of a glider winch launch", student research project at RWTH Aachen University, Dept. of Flight Dynamics, 2008. Available from: [darwin.bth.rwth-aachen.de/opus3/frontdoor.php?source\\_opus=3265](http://darwin.bth.rwth-aachen.de/opus3/frontdoor.php?source_opus=3265)
- <sup>3</sup>Eppler, R.: "Windenschlepp und optimale Ausklinhöhe", Draft available from: [www.daec.de/se/downloadfiles/2010/Windenstart\\_Prof\\_Eppler20100301.pdf](http://www.daec.de/se/downloadfiles/2010/Windenstart_Prof_Eppler20100301.pdf)
- <sup>4</sup>BGA Safety Initiative: "Safe Winch Launching", February 2010. Available from: [www.glidering.co.uk/bgainfo/safety/documents/safewinchbrochure-0210.pdf](http://www.glidering.co.uk/bgainfo/safety/documents/safewinchbrochure-0210.pdf)
- <sup>5</sup>Gäb, A., Nowack, J., and Alles, W.: "Requirements to servo-assisted control elements for sailplanes", *Technical Soaring*, Vol. 33, No. 1, 2009, pp. 21 – 27
- <sup>6</sup>Santel, C.: "An investigation of glider winch launch accidents utilizing multipoint aerodynamics models in flight simulation", diploma thesis at RWTH Aachen University, Dept. of Flight Dynamics, available from [darwin.bth.rwth-aachen.de/opus3/volltexte/2010/3454/](http://darwin.bth.rwth-aachen.de/opus3/volltexte/2010/3454/)
- <sup>7</sup>Williams, P., Lansdorp, B. and Ockels, W.: "Modeling and control of a kite on a variable length flexible inelastic tether", AIAA-2007-6705 in: AIAA Modeling and Simulation Technologies Conference, August 2007. Available from: [www.lr.tudelft.nl/live/pagina.jsp?id=fe263f84-29af-4010-8222-2f1112c8f223&lang=en&binary=/doc/Kite%20modelling%20flexible%20tether\\_bas.pdf](http://www.lr.tudelft.nl/live/pagina.jsp?id=fe263f84-29af-4010-8222-2f1112c8f223&lang=en&binary=/doc/Kite%20modelling%20flexible%20tether_bas.pdf)

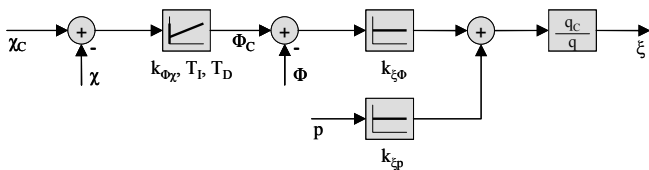


Figure 1 Schematic of the aileron controller channel

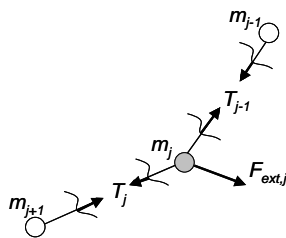


Figure 2 Forces at FEM element of cable

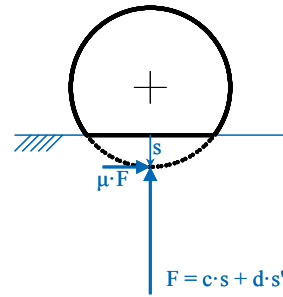


Figure 3 Ground reactions

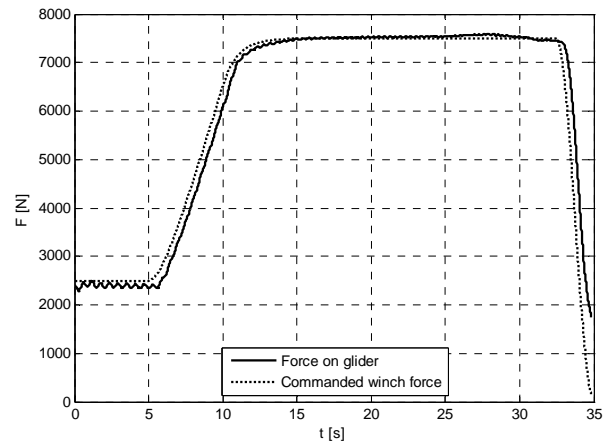


Figure 4 Reference launch cable force

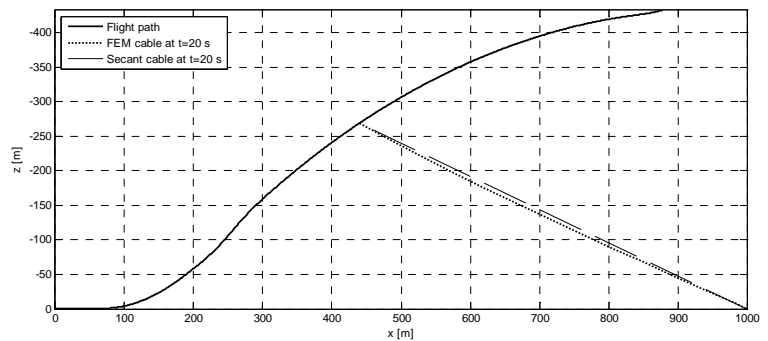


Figure 5 Reference launch flight path

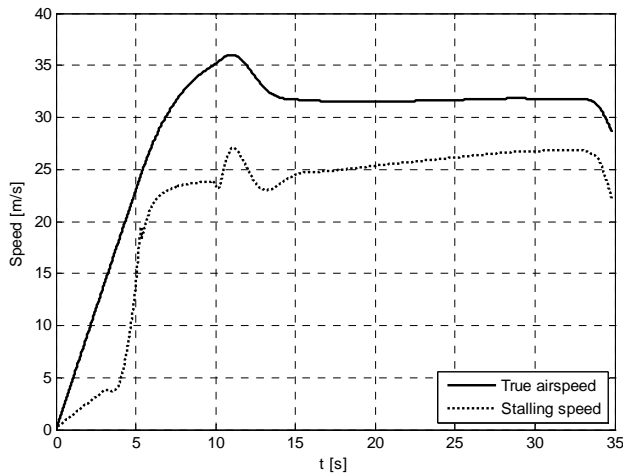


Figure 6 Reference case speeds

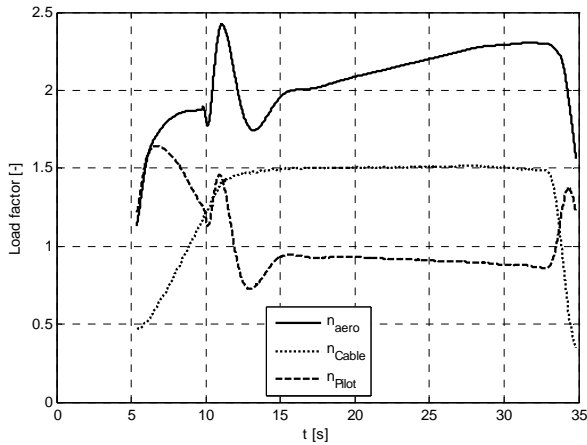


Figure 7 Reference launch load factors

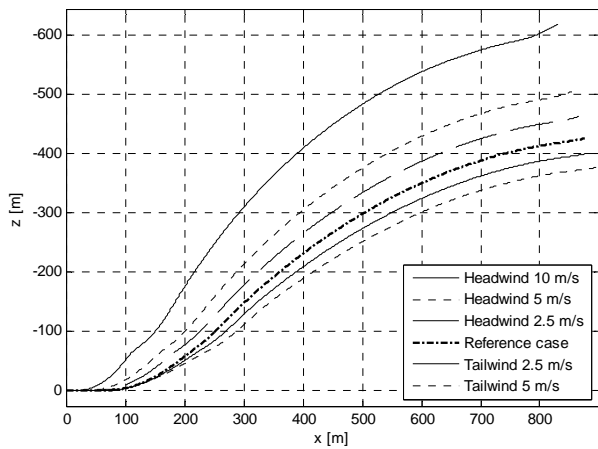


Figure 8 Flight paths with different longitudinal wind speeds

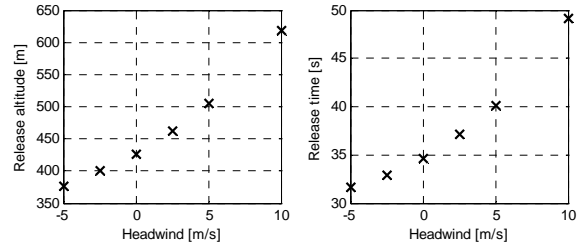


Figure 9 Release altitude and time with different wind speeds

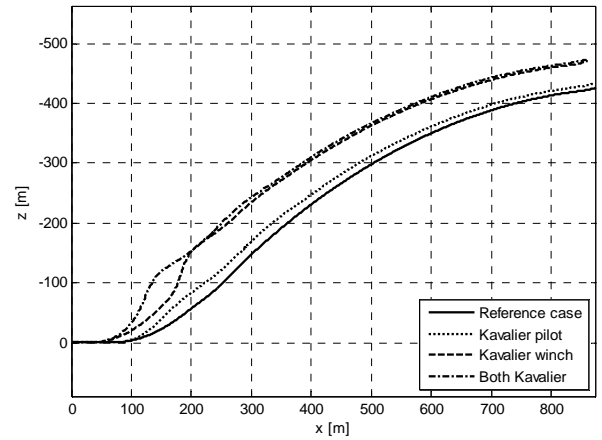


Figure 10 Flight paths in Kavalierstart

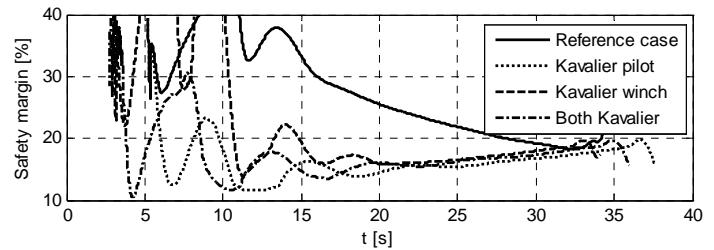
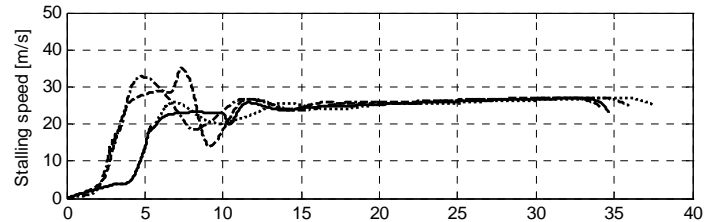
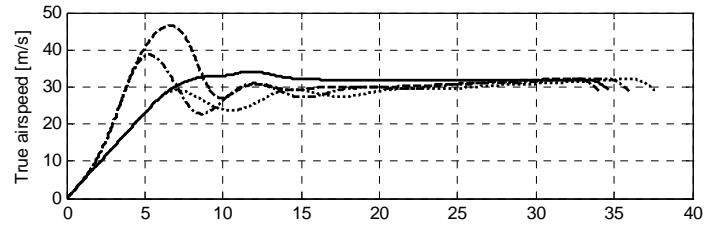


Figure 11 Speeds and safety margin in Kavalierstart